

The Significance of Pit Shape for Hydraulic Isolation of Embolized Conduits of Vascular Plants During Novel Refilling

W. KONRAD and A. ROTH-NEBELSICK*

Institut für Geowissenschaften, University of Tübingen, Sigwartstrasse 10, D-72076 Tübingen, Germany

*(*Author for correspondence, e-mail: anita.roth@uni.tuebingen.de)*

Abstract. During plant water transport, the water in the conducting tissue (xylem) is under tension. The system is then in a metastable state and prone to bubble development and subsequent embolism blocking further water transport. It has recently been demonstrated, that embolism can be repaired under tension (= novel refilling). A model (Pit Valve Mechanism = PVM) has also been suggested which is based on the development of a special meniscus in the pores (pits) between adjacent conduits. This meniscus is expected to be able to isolate embolized conduits from neighbouring conduits during embolism repair. In this contribution the stability of this isolating meniscus against perturbations is considered which inevitably occur in natural environments. It can be shown that pit shape affects the stability of PVM fundamentally in the case of perturbation. The results show that a concave pit shape significantly supports the stability of PVM. Concave pit shape should thus be of selective value for species practicing novel refilling.

Key words:

1. Introduction

According to the Cohesion-Tension Theory, upward water flow in land plants is generated by a water potential gradient driven by transpiring leaves [1, 2]. This mechanism can cause large tension gradients in the xylem, the water-conducting tissue of vascular plants [3–5]. Because it is in a metastable state, this system can be easily disturbed by the development of gas bubbles within these conduits, blocking transport of the water [6–8]. The water-transporting conduits of the xylem are tracheids or vessels formed by dead lignified cells with a typical radius of $30\ \mu\text{m} \dots 100\ \mu\text{m}$. The conduits are not laterally tight capillaries. Their walls are strewn with pores (=pits) which represent lateral channels between adjacent conduits. Water can flow through these pits from one conduit to a neighbour conduit. The pit channel between two adjacent conduits is separated by a porous membrane (=pit membrane) which represents the primary wall.

There are several possible mechanisms of bubble development during plant water transport [4, 9] It is, however, generally assumed that embolism events develop in many cases from an initially small, gas filled cavity in the xylem. This pre-existing bubble is drawn through the pores of the pit membrane into a functioning conduit (the “air seeding hypothesis,” [10]). The expansion of the gaseous space stops when the gas bubble reaches the conduit pits. This process leads to embolism preventing any further water transport. There is recent evidence that embolism occurs frequently during daily xylem water transport and can be removed (1) very quickly (within minutes) and (2) – at least in several species – under xylem tension, that is, during transpiration [11–14]. The last observation, termed as “novel refilling,” is difficult to explain [12, 15]. The following questions arise:

1. How is it possible that water moves into an embolized conduit when negative pressures exist in the adjacent functioning conduits? According to the pressure gradient (higher pressure in the embolized conduit than in the non-embolized conduits), water should rather flow out of the embolized conduit than into it.
2. How is it possible under these circumstances to achieve bubble dissolution in the embolized conduits, i.e. how can the positive pressures needed for refilling coexist with tension?
3. How is hydraulic continuity restored?

It has recently been suggested that (1) living cells within the xylem can supply embolized conduits with water needed for refilling [16] and (2) the surface properties and the pit geometry of the conduits cause interfacial effects which lead to hydraulic isolation and contribute to bubble dissolution [17]. This mechanism is termed as Pit Valve Mechanism (=PVM) throughout the rest of this paper. According to [17], novel refilling would thus rely on (1) a biological basis and (2) a physical basis represented by PVM. A biophysical analysis of PVM concentrating on the temporal course of bubble growth or bubble dissolution during embolism repair has been recently presented [18]. The essence of the repair scenario is that a “reverse meniscus” (see Figure 1) can develop between a gas bubble in the pit chamber (termed as “PB”, pit bubble, throughout the rest of this text) and the water in an embolized conduit if the contact angle and the geometry of the pit chamber are suitably related. The interface then exerts pressure upon the water and not upon the gas and is probably able to hydraulically isolate the embolized vessels from their intact neighbours, so that the high pressure required to drive the gas back into solution can be generated in the embolized conduit only. Although the study [18] demonstrated that PVM is principally possible there are still open questions concerning the reliability and biological relevance of PVM. One significant aspect is how stable PVM is against perturbations from external forces which inevitably occur in a natural environment (for example, mechanical vibrations caused by wind or animals) and how pit shape affects PVM. In this paper, the stability of PVM against perturbations and the influence of pit shape are investigated in detail. It will be demonstrated that pit shape is of high significance for the stability of PVM.

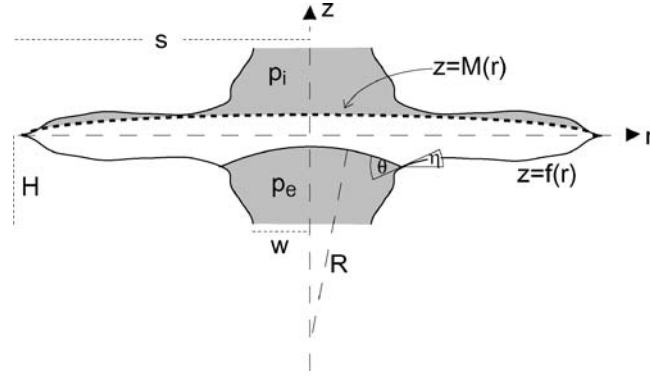


Figure 1. Section through a pit along its axis of symmetry. The shape of the pit is described by the function $z = f(\rho)$ (lower, right part of figure). The other parts of the pit shape arise from (1) mirror symmetry with respect to the $z = 0$ -plane (upper, right part of figure) and (2) rotational symmetry around the z -axis (left part of figure). The function $z = M(\rho)$ describes the membrane, which bends because of the pressure difference between the embolized vessel (pressure $p_e > 0$) and the intact vessel (pressure $p_i < 0$) towards the latter. θ denotes the contact angle between water and pit wall. η is the angle between the tangent of the function $f(\rho)$ and the $z = 0$ -plane, thus $\tan \eta = f'(\rho)$. s denotes the radius of the (unbent) pit membrane, w the radius of the pit mouth, and H the height of a half pit along its symmetry axis.

In the present article, we do not discuss PVM in general. For a general exposition as well as for the details of PVM we refer to [17, 18].

2. Concept of Stability for Axisymmetric Pit Bubbles

The reasoning in this section follows a line of thought given in Shen et al. [19] for spherically symmetric gas bubbles immersed in a liquid of either positive or negative pressure.

Our goal is to find a criterion which allows to decide whether or not a meniscus at a given position within a pit represents a point of stable or of unstable equilibrium with respect to small perturbations of the position of the meniscus.

If the gas bubble neither contracts nor expands, we may conclude that within the gas/liquid-interface an equilibrium exists between (1) the “confining” liquid pressure p_e , and (2) the “expansive” pressure \tilde{p} exerted by the expansion seeking gas within the bubble plus the surface tension of the reverse meniscus of the PB which acts, due to the pit geometry, also in an “expansive” way.

We start from the equation of an ideal gas

$$\tilde{p} = \frac{\mathcal{R}T n}{V} \quad (1)$$

and from the Young–Laplace Equation

$$p = p_e - \frac{2\gamma}{R} \quad (2)$$

where the quantity R denotes the radius of curvature of the meniscus (the geometry is depicted in Figure 1) and expand \tilde{p} and p in Taylor series with respect to V around the equilibrium value $V = V_0$,

$$\tilde{p}(V_0 + dV) = \tilde{p}(V_0) - \frac{\mathcal{R}T n}{V_0^2} dV + (\text{terms of order } (dV)^2 \text{ and higher}) \quad (3)$$

$$p(V_0 + dV) = p(V_0) + \frac{2\gamma}{R_0^2} \left. \frac{dR}{dV} \right|_0 dV + (\text{terms of order } (dV)^2 \text{ and higher}) \quad (4)$$

Retaining only terms linear in dV , we obtain

$$\begin{aligned} \delta p := \tilde{p}(V_0 + dV) - p(V_0 + dV) &= \{\tilde{p}(V_0) - p(V_0)\} \\ &\quad - \left[\frac{\mathcal{R}T n_0}{V_0^2} + \frac{2\gamma}{R_0^2} \left. \frac{dR}{dV} \right|_0 \right] dV \end{aligned} \quad (5)$$

The expression in the braces in Equation (5) disappears because of the assumed equilibrium at $V = V_0$, i.e. $\tilde{p}(V_0) = p(V_0)$.

For an interpretation of Equation (5) recall that δp denotes the discrepancy between expansion and contraction seeking pressures which develop after a disturbance connected with a volume change dV . Simplifying the terms in the brackets with Equations (1) and (2) and applying the definition

$$\xi := \left[\frac{1}{V} \left(p_e - \frac{2\gamma}{R} \right) + \frac{2\gamma}{R^2} \left. \frac{dR}{dV} \right|_0 \right] \quad (6)$$

(each quantity is to be evaluated at its equilibrium value, denoted by the index 0), Equation (5) reads as

$$\delta p = -\xi dV \quad (7)$$

On inspection of Equation (7) we notice that two cases may be realized:

1. $\xi > 0$: In this case, an increase in bubble volume (i.e. $dV > 0$) implies $\delta p < 0$. That is, the initial (externally caused) increase in volume makes the contracting forces dominate the expanding forces, whereupon the bubble volume V returns to its equilibrium value V_0 , provided, the system is undisturbed afterwards. A decrease in bubble volume (i.e. $dV < 0$), however, implies $\delta p > 0$, hence the bubble volume is expanded to the equilibrium value from which it was ‘‘perturbed away’’. Thus, if $\xi > 0$, equilibrium is restored irrespective of the sign of the perturbation dV .
2. $\xi < 0$: In this case, $dV > 0$ implies $\delta p > 0$ and $dV < 0$ implies $\delta p < 0$. The consequences are quite different from the previous case, because an increase in bubble volume ($dV > 0$) now leads to a strengthening of the expanding forces ($\delta p > 0$) leading to a further bubble expansion. Similarly, an initial decrease of

bubble radius reinforces the contracting forces resulting in a further contraction of the bubble, etc. Thus, once the equilibrium has been perturbed, it will never be restored.

From Equation (6) we draw the conclusions:

1. If p_e (the liquid pressure in the embolized conduit) is high enough, every pit bubble exhibits stable equilibrium.
2. As the difference $p_e - (2\gamma/R)$ represents via the Young-Laplace-Equation (2) the (necessarily positive) pressure in the PB, $dR/dV > 0$ implies $\xi > 0$. For $dR/dV < 0$, however, ξ may be positive or negative, depending on the absolute value of dR/dV . Thus, $dR/dV > 0$ is sufficient (although not necessary) for stability.

Further conclusions require more explicit prescriptions of the geometry of the pits to be investigated.

3. Pit Shape – General Considerations

Small variations in shape have a profound influence on stability, precise data of the morphology of pits are, however, difficult to obtain. Therefore, we approach the problem of PB stability from a more theoretical point of view: we apply the stability criterion Equation (7) to several “typical” but idealized pit forms and try to identify pit shapes which are able to support stability of PVM. Support for approach comes from the principle of natural selection which suggests that pit shapes fulfilling the stability criterion are more likely expressed by plants than those failing in this respect, provided, that embolism repair actually takes place and if stability in the sense defined above is a necessary prerequisite for it.

For the sake of simplicity, we assume axial symmetry of the pits (with the axis normal to the pit membrane) because then, any liquid/gas-interface figures as a section of a sphere of radius R . Figure 1 shows a pit connecting an intact (upper part of figure) and an embolized (lower part of figure) vessel. We introduce coordinates r (the distance from the symmetry axis) and z (identical with the symmetry axis).

The shape of the pit is described by the function $z = f(r)$ and, s , the radius of the (unbent) pit membrane, w , the radius of the pit mouth, and H , the height of a half pit along its symmetry axis. θ is the contact angle between water and pit wall. Finally, η denotes the angle between the tangent of the function $f(r)$ and the $z = 0$ -plane, thus $\tan \eta = f'(r)$. $z = M(r)$ describes the shape of the membrane which is possibly bent towards the upper part of the pit.

The radius R of the meniscus developing in the lower part of the pit and the gas volume between meniscus and pit membrane can be calculated quite generally, if the contact angle θ and the pit shape $z = f(r)$ are given (and if $f(r)$ behaves sensible). Employing the definitions of the quantities θ and η , we infer with standard methods

of geometry for a meniscus touching the pit wall at position $(r, z) = (\rho, -\zeta)$:

$$R(\rho) = \frac{\rho}{\sin(\theta - \eta(\rho))} = \frac{\rho \sqrt{1 + f'(\rho)^2}}{\sin \theta - f'(\rho) \cos \theta} \quad (8)$$

Similarly, from formulas of trigonometry, the height $g(\rho)$ (measured along the z -axis) of the spherical segment denoted V_{kal} in Figure 2 is calculated as

$$g(\rho) = R(\rho)[1 - \cos(\theta - \eta)] = R(\rho) \left[1 - \frac{\cos \theta + f'(\rho) \sin \theta}{\sqrt{1 + f'(\rho)^2}} \right] \quad (9)$$

From Figure 2 it is apparent that the gas volume $V(\rho)$ within the PB can be obtained via $V = V_{\text{mem}} + V_{\text{int}} - V_{\text{kal}}$.

1. The volume V_{kal} follows from geometrical formulas related to spheres:

$$V_{\text{kal}}(\rho) = \frac{\pi}{3} g(\rho)^2 [3 R(\rho) - g(\rho)] \quad (10)$$

2. V_{int} is calculated by cutting the volume into a stack of circular discs of radius $r(z)$ and of thickness dz , sharing the problem's symmetry around the z -axis. The connection between the z -position and the radius r of each disc is provided by the relation $z = f(r)$, hence,

$$V_{\text{int}}(\rho) = \pi \int_{-\zeta}^0 f^{-1}(z) dz \quad (11)$$

where the integration is from $z = -\zeta$ (where the meniscus touches the pit wall) till the $z = 0$ -plane. Application of the substitution rule of integration with respect to the relation $z = f(r)$ implies $dz = f'(r) dr$ (a prime denotes differentiation with respect to the argument), $f^{-1}(-\zeta) = \rho$ and $f^{-1}(0) = f(s)$,

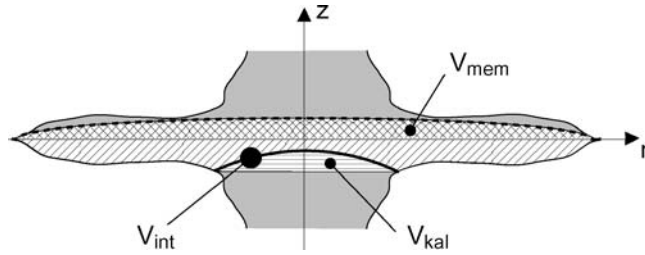


Figure 2. Volumes involved in the calculation of the gas volume within the pit (Equations (10) through (14)). Oblique cross hatching (V_{mem}) denotes the gas volume between the $z = 0$ -plane and the distorted pit membrane, simple oblique hatching ($V_{\text{int}} - V_{\text{kal}}$) denotes the gas volume between the $z = 0$ -plane and the gas/liquid interface and horizontal hatching designates the spherical segment V_{kal} . V_{kal} is filled with liquid, *not* with gas.

provided f is a one-to-one function. If so, V_{int} takes the form

$$V_{\text{int}}(\rho) = \pi \int_{\rho}^s r^2 f'(r) dr \quad (12)$$

The examples of the relation $z = f(r)$ we shall calculate below, are one-to-one functions.

3. V_{mem} is calculated similarly as V_{int} by exploiting first its symmetry with respect to the z -axis

$$V_{\text{mem}}(\rho) = \pi \int_0^{M(0)} r^2 dz = \pi \int_s^0 r^2 M'(r) dr \quad (13)$$

and then using the substitution rule of integration with respect to the relation $z = M(r)$.

Collecting these contributions we arrive eventually at

$$\begin{aligned} V(\rho) &= V_{\text{int}}(\rho) - V_{\text{kal}}(\rho) + V_{\text{mem}}(\rho) \\ &= \pi \int_{\rho}^s r^2 f'(r) dr - \frac{\pi}{3} g(r)^2 [3R(r) - g(r)] + \pi \int_s^0 r^2 M'(r) dr \quad (14) \end{aligned}$$

The ‘‘typical’’ pit forms we will consider share the following geometric properties: (1) the radius s of the (unbent) membrane, (2) the ‘‘mouth radius’’ w , and (3) the half height H (as measured along the symmetry axis). Thus, a curve $z = f(r)$ describing the pit shape has to pass through the points $(r, z) = (s, 0)$ and $(r, z) = (w, -H)$.

4. Shape of the Pit Membrane

Before proceeding with the analysis of the influence of pit shape on the stability of PVM, we have to consider the shape of the pit membrane. In a pit connecting two intact vessels, the membrane should be unbent, i.e. coincide with the plane $z = 0$. After an embolism has occurred and a PB isolates intact and embolized vessel from each other, the former vessel remains under negative pressure (typically $p_i \approx -4 \text{ MPa} \dots -1 \text{ MPa}$) whereas the pressure p_e within the latter increases to a positive value, probably close to atmospheric pressure (i.e. $p_e \approx 0.1 \text{ MPa}$), as explained in the introduction. The membrane therefore bulges towards the intact vessel and assumes the shape $z = M(r)$. In SEM pictures, deformed pit membranes can be observed [20]. Additionally, there are indications of pit membrane fatigue after embolism events due to strong mechanical load and deformation [21]. Thus, deviations from the original (unbent) shape of the pit membrane have to be taken into account.

We will now explore which shape of a bent pit membrane is appropriate, because the function $z = M(r)$ which contributes to the expression $V(r)$ for the gas

volume in the pit (Equation (13)) has to be determined as a prerequisite for calculating ξ (Equation (6)). The appropriate way to treat this situation would be to calculate the shape of the membrane caused by the pressure difference from the elasto-mechanical properties of pit membranes. Because these are – to the authors knowledge – not known, we examine two somewhat idealized cases that can be treated without this information.

1. We consider a very stiff membrane that remains in the $z = 0$ -plane in spite of the pressure difference trying to bend it, i.e.

$$M(r) = 0 \quad (15)$$

2. For the sake of simplicity, we assume only the central part of the membrane to be undeformably stiff; its periphery, however, we assume to be very elastic. Then, the pressure difference pushes the membrane along the positive z -axis until its elastic periphery clings to the pit wall (described by the function $z = f(r)$) and the central part is located on the pit opening towards the intact vessel like a flat lid:

$$M(r) = \begin{cases} -f(w) & \text{if } 0 \leq r \leq w \\ -f(r) & \text{if } w \leq r \leq s \end{cases} \quad (16)$$

In both cases, the gas volume above the $z = 0$ -plane contributes to $V(r)$ (as calculated in Equation (13)) only a constant term which is independent of the coordinate r and vanishes therefore from the derivative dV/dr . Thus, in the treatment we are going to apply, the second term in ξ (Equation (6)) is not affected by the reaction of the membrane to changes in the pressure difference of the gaseous content of the PB which occur after the event of embolism has taken place. The contribution of $M(r)$ to the first term in ξ (via $V(r)$) can be easily calculated.

5. Pit Shape – Examples

There is an infinity of shape-defining curves. We choose to describe curved pit walls by

$$f(r) = z_0 + \frac{b}{a} \sqrt{a^2 - (r_0 - r)^2} \quad (17)$$

which is part of an ellipse with centre $(r, z) = (r_0, z_0)$ and long and short half axes a and b , respectively (see Figure 3).

Four conditions are necessary to determine the four constants r_0, z_0, a and b . Two of them are derived from the condition that the pit curve should have its endpoints at $(r, z) = (s, 0)$ and $(r, z) = (w, -H)$. Insertion of these into Equation (17) gives

$$0 = f(s) = z_0 + \frac{b}{a} \sqrt{a^2 - (r_0 - s)^2} \quad (18)$$

$$-\frac{H}{2} = f(w) = z_0 + \frac{b}{a} \sqrt{a^2 - (r_0 - w)^2} \quad (19)$$

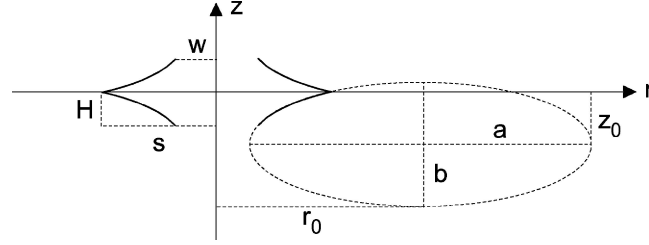


Figure 3. Pit, generated by rotating part of an ellipse around the symmetry axis of the pit, i.e. the z -axis. The general features of the pit shape are defined by the quantities s , w and H . Its detailed features are described by a section of the ellipse of Equation (17), which contains the four constants r_0 , z_0 , a and b . By adjusting their values appropriately, the real pit shape can be approximated.

The remaining two constants follow from other conditions: we could demand, for instance, that $f(r)$ touches two more prescribed points. Alternatively, we require $f(r)$ to form the angle η_s with the $z = 0$ -plane at the point $r = s$ and, likewise, the angle η_w with the $z = -H$ -plane at $r = w$. Employing Equation (17) this amounts to

$$\tan \eta_s = f'(s) = \frac{b}{a} \frac{r_0 - s}{\sqrt{a^2 - (r_0 - s)^2}} \quad (20)$$

$$\tan \eta_w = f'(w) = \frac{b}{a} \frac{r_0 - w}{\sqrt{a^2 - (r_0 - w)^2}} \quad (21)$$

Calculation of r_0 , z_0 , a and b from the system of Equations (18) to (21) completes pit shape determination.

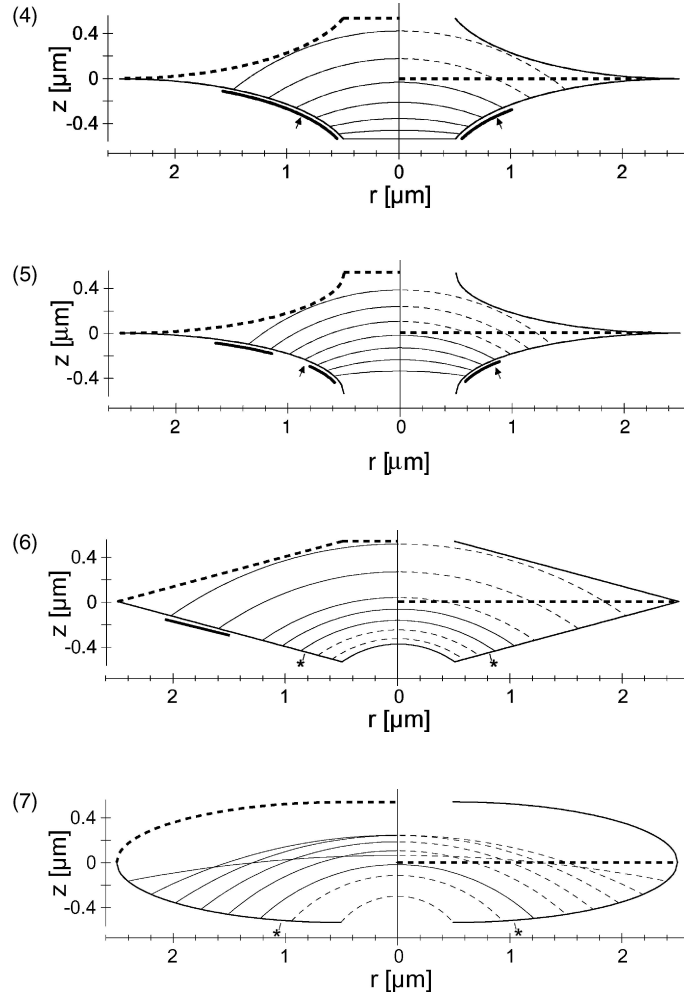
We now consider four different pit forms. Three of them (Figures 4, 5 and 7) are derived from (17) by choosing specific values for η_s and η_w , the fourth one (Figure 6) is generated by rotating a straight line around the symmetry axis of the pit.

Concave pit (a), Figure 4 ($\eta_s = 0$, $\eta_w = \theta$):

$$f(r) = -\frac{H}{s - w - 2H \cot \theta} \left(s - w - H \cot \theta - \sqrt{(s - w - H \cot \theta)^2 - (s - r)^2 \left(1 - \frac{2H \cot \theta}{s - w} \right)} \right) \quad (22)$$

Concave pit (b), Figure 5 ($\eta_s = 0$, $\eta_w = \pi/2$):

$$f(r) = -\frac{H}{s - w} (s - w - \sqrt{(s - w)^2 - (s - r)^2}) \quad (23)$$



Figures 4–7. The four pit shapes of Equations (22) to (25) (for orientation see also Figure 1).

- Upper pits open into intact, lower pits open into embolized vessels.
- Right halves of the figures are related to a very stiff, immovable membrane (Equation (15)), left halves correspond to a partially stiff, partially elastic membrane adapting to the shape of the pit wall (Equation (16)).
- Membranes are indicated by thick, broken lines.
- Sectors of circles represent liquid/gas-interfaces. Thin, broken lines indicate interfaces which cannot exist, because they would touch the membrane (higher r -values, all figures) or because they imply negative pressures in the PB (lower r -values, between asterisks in Figure 6 [$r_* = 0.83 \mu\text{m}$] and Figure 7 [$r_* = 1.03 \mu\text{m}$]).
- Thick black strokes beneath the pit walls indicate possible positions of stable interfaces.
- Arrows point to minima of the interface radii of curvature $R(r)$ in Figure 4 ($r_{\nearrow} = 0.89 \mu\text{m}$) and Figure 5 ($r_{\nearrow} = 0.85 \mu\text{m}$).
- Values common to all figures: radius of pit membrane $s = 2.5 \mu\text{m}$, radius of pit mouth $w = 0.5 \mu\text{m}$, half height of pit $H = 0.54 \mu\text{m}$, pressure within embolized vessel $p_e = 100\,000 \text{ Pa}$ (cf. Figure 1). All interfaces form the same contact angle ($\theta = 50^\circ$) with the pit wall.

Straight walled pit, Figure 6:

$$f(r) = -\frac{H}{s-w}(s-r) \quad (24)$$

Convex pit, Figure 7 ($\eta_s = \pi/2$, $\eta_w = 0$):

$$f(r) = -\frac{H}{s-w}(\sqrt{(s-w)^2 - (r-w)^2}) \quad (25)$$

The range of r is in all cases restricted to

$$w \leq r \leq s \quad (26)$$

6. Application of Stability Criterion – Effects of Pit Shape on PVM

Insertion of the definitions of pit and membrane shape (Equations (22) to (25) and Equations (15) or (16)) into Equations (8) to (9) allows explicit calculation of $R(r)$, $V(r)$ and $\xi(r)$. We do not give here the resulting, rather lengthy expressions, because the main results can be more easily obtained from Figures 4–7. These have been calculated for the following (common) values: Contact angle between interfaces and pit wall: $\theta = 50^\circ$, radius of pit membrane: $s = 2.5 \mu\text{m}$, radius of pit mouth: $w = 0.5 \mu\text{m}$, height of pit: $H = 0.54 \mu\text{m}$, pressure within embolized vessel: $p_e = 100\,000 \text{ Pa}$.

Before inspecting the results, we summarize conditions which are to be satisfied by successfully operating gas/liquid-interfaces:

1. Interfaces should bulge towards the intact vessel, that is, every interface at position $r = \rho$ should obey the inequality $\theta > \eta(\rho) = \arctan f'(\rho)$ (cf. Figure 1).
2. An interface should not touch the membrane, as otherwise water molecules from both sides of the membrane would come into contact, and the conductivity of the xylem sap through the membrane would be restored. This would lead to a breakdown of hydraulic isolation.
3. An interface should be stable, i.e. the inequality $\xi(\rho) > 0$ should be fulfilled for an interface at position ρ .
4. Being filled by a gas, the pressure in the PB should be positive. The condition $p > 0$ implies via the Young-Laplace Equation (2), $R(\rho) > 2\gamma/p_e \approx 1.44 \mu\text{m}$. The numerical value is obtained upon insertion of $p_e = 100\,000 \text{ Pa} \approx p_{\text{atm}}$.

Conditions (1) and (2) are related solely to geometric properties of a pit, whereas (3) and (4) also include the liquid pressure p_e in the embolized vessel.

It should be noted at this point that the results concerning stability presented so far, do apply not only to gas bubbles which consist solely of air molecules but also to bubbles including water vapour. This is possible because the underlying principles

of the model considerations presented above are not restricted to a special gas (apart from the assumption that they can be treated as an ideal gas).

In the following, the results depicted in Figures 4–7 will be analyzed with respect to the suitability of the different pit shapes for PVM. The degree of suitability is reflected by the ability of the pit shape to maintain stability of hydraulic isolation by obeying conditions (1)–(4).

We recall that the first term in ξ (Equation (6)) is necessarily (independent of pit shape) positive, if condition (4) is fulfilled. The second term in ξ , however, can attain both signs: for $dR/dV > 0$ it is positive, for $dR/dV < 0$ it is negative. Thus, the second term in ξ is shape-dependent, not in a very obvious way but – because of $dR/dV = (dR/d\rho)/(dV/d\rho)$ – rather through the ρ -dependance of the radius of curvature of the liquid/gas-interface $R(\rho)$ and of the gas volume $V(\rho)$.

The different degrees of suitability of the pit shapes of Figures 4–7 for maintaining stability during perturbation can be summarized as follows:

- Since all conditions apply, the concave pit with $\eta_w = \theta$ (Equation (22), Figure 4) is best suited to maintain stability of hydraulic isolation of an embolized vessel, at least for the parameter values given above. Notice, that for ρ -values between the arrows in Figure 4 the relation $dR/dV > 0$ holds, hence both terms in ξ are positive. ρ -values beyond the arrows are connected with $dR/dV < 0$, thus the second term in ξ is negative. Altogether, however, $\xi > 0$ is valid and stability is maintained.
- The concave pit with $\eta_w = 0$ (Equation (23), Figure 5) is very similar to the concave pit with $\eta_w = \theta$. The only difference lies in the “stability gap” in the case of the partially elastic membrane (left half of Figure 5), which opens up because the balance between the positive first and negative second term in ξ is in this case more delicate.
- The pit with straight walls (Equation (24), Figure 6) exhibits stability only if the membrane is – at least partially – elastic. This can be understood as follows: The derivative $dR/dV = (dR/d\rho)/(dV/d\rho)$ is negative for all interfaces (as can be seen from inspection of Figure 6: obviously, $dV/d\rho$ is a decreasing function of ρ , whereas $dR/d\rho$ increases with ρ). Therefore, stability is restricted to ρ -values for which the gas volume $V(\rho)$ is comparatively small, and the first, positive, term in ξ becomes – due to its $1/V(\rho)$ -dependancy – larger than the second, negative term. Figure 6 (left half of Figure) shows that this occurs with higher ρ -values of the elastic membrane, because then the fluid/gas-interface lies relatively close to the upper pit wall, thus leaving little gas space $V(\rho)$.

In contrast, the gas volume between the stiff membrane and an interface close to it (right part of Figure 6) is much larger and diminishes the positive first term in ξ to such an extent that ξ as a whole remains below zero. Comparison with the concave interfaces in Figures 4 and 5 reveals that straight walls are unfavourable with respect to minimizing the gas volume $V(\rho)$.

We note that interfaces with $r \leq 0.83 \mu\text{m}$ (indicated by an asterisk in the figure) generally violate condition (4) (the pressure in the PB should be positive) and therefore cannot exist.

- The convex pit (Equation (25), Figure 7) does not allow for stability since the derivative dR/dV is negative for all interfaces and the sum of both terms in ξ is negative even for a partially elastic membrane.

7. Concluding Remarks

The results of these theoretical studies demonstrate the significance of detailed pit shape for the functionality of PVM. Additionally to the basic prerequisite architecture – the funnel-shaped appearance – concave curvature of the pit chamber is beneficial for PVM, because it leads to the maintenance of the hydraulic isolation of the embolized pit under mechanical perturbations, which will inevitably occur in a natural environment (e.g. wind, animals). This effect is not restricted to a special gas and is thus applicable to both air and water vapour bubbles. As is also demonstrated in this study, the deformation of the pit membrane due to the strong pressure difference between functioning and embolized conduits also contributes to the stability of PVM. Hence, it may be speculated that interfacial effects in wood play a significant functional role in plant water transport under various aspects.

From this we draw the conclusion that PVM – if it is biologically relevant – should lead to concave pit shapes by natural selection. In order to verify this hypothesis, it will be necessary to collect detailed information about the shapes of real pits, preferably from SEM-pictures of undistorted xylem vessels of various species.

Further research should also address the possible functional implications of the numerous microstructures which are expressed by wood conduits, because the above results indicate that at least some of them may be involved in interfacial effects. Combined studies concerning physical, anatomical and ecophysiological aspects are expected to contribute significantly to our knowledge of fluid behaviour in wood on the micrometer/nanometer scale.

Acknowledgements

We thank the Federal State of Baden-Württemberg for partly supporting this study within the framework of the Competence Network “Biomimetics.” We thank James Nebelsick for carefully reading the manuscript.

Note Added in Proof

During the publication procedure of this manuscript, a new paper was published by Salleo et al. (2004) in which (1) novel refilling in *Laurus nobilis* L. was again confirmed and (2) the refilling process was interpreted to be dependent on living cells.

S. Salleo, Lo Gullo, M.A., Trifilo, P. and Nardini, A.: New evidence for a role of vessel-associated cells and phloem in the rapid xylem refilling of cavitated stems of *Laurus nobilis* L. *Plant Cell Environ.* **27** (2004), 1065–1076.

References

1. Tyree, M.T. and Ewers, F.: The Hydraulic Architecture of Trees and Other Woody Plants, *New Phytol.* **199** (1991), 345–360.
2. Zimmermann, M.H.: *Xylem Structure and the Ascent of Sap*, Springer-Verlag: Berlin (1983).
3. Holbrook, N.M., Ahrens, E.T., Burns, M.J. and Zwieniecki, M.A.: *In Vivo* Observation of Cavitation and Embolism Repair Using Magnetic Resonance Imaging, *Plant Physiol.* **126** (2001), 27–31.
4. Pickard, W.F.: The Ascent of Sap in Plants, *Prog. Biophys. Mol. Biol.* **37** (1981), 181–229.
5. Pockman, W.T., Sperry, J.S. and OLeary, J.W.: Sustained and Significant Negative Water Pressure in Xylem, *Nature* **378** (1995), 715–716.
6. Milburn, J.A.: Cavitation and Embolisms in Xylem Conduits, in A.S. Raghavendra (ed.) *Physiology of Trees*, Wiley: New York (1991), pp. 163–174.
7. Tyree, M.T. and Sperry, J.S.: The Vulnerability of Xylem to Cavitation and Embolism, *Annu. Rev. Plant Physiol., Plant Mol. Biol.* **40** (1989), 19–38.
8. Tyree, M.T. and Yang, S.: Water-Storage Capacity of *Thuja*, *Tsuga* and *Acer* Stems Measured by Dehydration Isotherms: The Contribution of Capillary Water and Cavitation, *Planta* **182** (1990), 420–426.
9. Hölttä, T., Vesala, T., Perämäki, M. and Nikinmaa, E.: Relationships Between Embolism, Stem Water Tension and Diameter Changes, *J. Theor. Biol.* **215** (2002), 23–38.
10. Sperry, J.S. and Tyree, M.T.: Mechanism of Water Stress-Induced Xylem Embolism, *Plant Physiol.* **88** (1988), 581–587.
11. Bucci, S.J., Scholz, F.G., Goldstein, G., Meinzer, F.C., Sternberg, L. and Da, S.L.: Dynamic Changes in Hydraulic Conductivity in Petioles of Two Savanna Tree Species: Factors and Mechanisms Contributing to the Refilling of Embolized Vessels, *Plant Cell Environ.* **26** (2003), 1633–1645.
12. Hacke, U.G. and Sperry, J.S.: Limits to Xylem Refilling Under Negative Pressure in *Laurus nobilis* and *Acer negundo*, *Plant Cell Environ.* **26** (2003), 303–311.
13. Salleo, S., LoGullo, M., Depaoli, M. and Zippo, M.: Xylem Recovery from Cavitation-Induced Embolism in Young Plants of *Laurus nobilis*: A Possible Mechanism, *New Phytol.* **132** (1996), 47–56.
14. Tyree, M.T., Salleo, S., Nardini, A., LoGullo, M.A. and Mosca, R.: Refilling of Embolized Vessels in Young Stems of Laurel: Do We Need a New Paradigm? *Plant Physiol.* **120** (1999), 11–21.
15. Steudle, E.: The Cohesion-Tension Mechanism and the Acquisition of Water by Plant Roots, *Annu. Rev. Plant Physiol., Plant Mol. Biol.* **52** (2001), 847–875.
16. Vesala, T., Hölttä, T., Perämäki, M. and Nikinmaa, E.: Refilling of a Hydraulically Isolated Embolized Xylem Vessel: Model Calculations, *Ann. Bot.* **91** (2003), 419–428.
17. Holbrook, N.M., Zwieniecki, M.A.: Embolism Repair and Xylem Tension. Do we need a Miracle? *Plant Physiol.* **120** (1999), 7–10.
18. Konrad, W. and Roth-Nebelsick, A.: The Dynamics of Gas Bubbles in Conduits of Vascular Plants and Implications for Embolism Repair, *J. Theor. Biol.* **224** (2003), 43–61.
19. Shen, F., Gao, R., Liu, W. and Zhang, W.: Physical Analysis of the Process of Cavitation in Xylem Sap, *Tree Physiol.* **22** (2002), 655–659.
20. Wheeler, E.A.: Intervascular Pit Membranes in *Ulmus* and *Celtis* Native to the United States, *IAWA Bulletin* **4** (1983), 79–88.

21. Hacke, U.G., Stiller, V., Sperry, J.S., Pittermann, J. and McCulloh, K.A.: Cavitation Fatigue. Embolism and Refilling Cycles Can Weaken the Cavitation Resistance of Xylem, *Plant Physiology* **125** (2001), 779–786.
22. Carlquist, S.: *Comparative Wood Anatomy*, Berlin, Heidelberg, New York, 2001.
23. Cochard, H., Ewers, F. and Tyree, M.T.: Water Relations of a Tropical Vinelike Bamboo (*Rhipidocladum racemiflorum*): Root Pressures, Vulnerability to Cavitation and Seasonal Changes in Embolism, *J. Exp. Bot.* **45** (1994), 1085–1089.
24. Ewers, F.W., Fisher, J.B. and Fichtner, K.: Water Flux and Xylem Structure in Vines, in F.E. Putz and H.A. Mooney (eds.) *The Biology of Vines*, Cambridge University Press, Cambridge (1991), pp. 127–160.
25. Fisher, J.B., Angeles, G., Ewers, F.W. and Lopez-Portillo, J.: Survey of Root Pressure in Tropical Vines and Woody Species, *Int. J. Plant Sci.* **158** (1997), 44–50.
26. Lösch, R.: Wasserhaushalt der Pflanzen. Quelle und Meyer (2001), Wiebelsheim.
27. Magnani, F. and Borghetti, M.: Interpretation of Seasonal Changes of Xylem Embolism and Plant Hydraulic Resistance, *Plant Cell Environ.* **18** (1995), 689–696.
28. Tyree, M.T., Fiscus, E.L., Wullschleger, S.D. and Dixon, M.A.: Detection of Xylem Cavitation in Corn Under Field Conditions, *Plant Physiol.* **82** (1986), 597–599.
29. Yang, S. and Tyree, M.T.: A Theoretical Model of Hydraulic Conductivity Recovery From Embolism With Comparison to Experimental Data on *Acer saccharum*, *Plant Cell Environ.* **15** (1992), 633–643.
30. Zwieniecki, M.A. and Holbrook, N.M.: Bordered Pit Structure and Vessel Wall Surface Properties. Implications for Embolism Repair, *Plant Physiol.* **123** (2000), 1015–1020.
31. Zwieniecki, M.A., Melcher, P.J. and Holbrook, N.M.: Hydraulic Properties of Individual Xylem Vessels of *Fraxinus americana*, *J. Exp. Bot.* **52** (2001), 257–264.